

Symmetrical 1,2-Phenylenediamine Schiff's Base Derivatives as New Potential Dna Intercalators

Nisreen H Meiqal ¹, Sofian S. Mohamed ², Shahrazad Ali Eteer ¹, Jamal Ali M Elbakay ¹, Inass A Sadawe ¹, Salah M Bensaber ¹, Amira A. Gbaj ¹, Anton Hermann ³, Massaud Salem Maamar ⁴, and Abdul M Gbaj ^{1*}

¹Department of Medicinal Chemistry, Faculty of Pharmacy, University of Tripoli, Tripoli, Libya.

²Department of Chemistry and Toxins, Judicial Expertise and Research Center, Tripoli, Libya.

³Department of Biosciences, University of Salzburg, Salzburg, Austria.

⁴Zoology Department, Faculty of Science, Tripoli University, Tripoli, Libya.

***Corresponding Author:** Abdul M Gbaj, Professor of Genetics and Biochemistry, Department of Medicinal Chemistry, Faculty of Pharmacy, University of Tripoli, Libya.

Received Date: August 02, 2024; **Accepted Date:** August 13, 2024; **Published Date:** August 20, 2024

Citation: Nisreen H Meiqal, Sofian S. Mohamed, Shahrazad Ali Eteer, Jamal Ali M Elbakay, Inass A Sadawe, et al. (2024), Symmetrical 1,2-Phenylenediamine Schiff's Base Derivatives as New Potential Dna Intercalators, *J. Surgical Case Reports and Images* 7(7); DOI: [10.31579/2690-1897/209](https://doi.org/10.31579/2690-1897/209)

Copyright: © 2024, Abdul M Gbaj. This is an open access article distributed under the Creative Commons Attribution License, which permits unrestricted use, distribution, and reproduction in any medium, provided the original work is properly cited.

Abstract

Fifteen symmetrical 1,2-phenylenediamine Schiff's base derivatives were designed as DNA intercalators. Adsorption, distribution, metabolism, elimination, and toxicity (ADMET) properties and drug-likeness of the designed compounds were predicted by Swiss-ADME software, and the molecular docking study was performed in the PyRx tool. Four Compounds NHM01, NHM04, NHM06 and NMH11 were synthesized and the structure of each compound was analyzed using Fourier transform infrared spectroscopy (FTIR), ¹H NMR and ¹³C NMR. Moreover, the four compounds were in vitro biologically screened for their interactions with the genomic DNA. The binding properties of these compounds to genomic DNA (G-DNA) were investigated by UV-visible absorption and fluorescence spectroscopy. The molecular docking studies of compounds revealed that all the compounds are bioactive, however, compound NHM01 shows significant DNA binding affinity over standard drugs. The biological results indicate that the four synthesized compounds can interact with G-DNA by intercalation binding. Compound NHM01 showed the highest key selection vector (KSV) value, followed by NHM04, which suggests that compound NHM01 binds most tightly to G-DNA. Our results demonstrate that NHM01 and NHM04 may serve as novel lead compounds for the discovery of more 1,2-phenylenediamine Schiff's base derivatives with improved anticancer potency and selectivity.

Keywords: schiff's base; dna intercalator; anticancer; ortho-phenylenediamine; molecular docking

1. Introduction

Deoxyribonucleic acid (DNA) is the storage unit of genetic information and considered as major biological target for numerous anticancer agents. The anticancer agents that target DNA generally interact with DNA through reversible binding by three main modes: static electronic interactions, groove binding, or intercalation. The static electronic interactions (external surface binding) could be related to the cationic molecules that bind non-specifically with the anionic sugar phosphate backbone of DNA through outer edge stacking (Serec et al., 2016). The second mode of interaction is groove binding which comprises the insertion of the molecule into the base edges of the minor or major groove (usually G•C sites in the major groove, A•T sites in the minor groove). The

major groove has multiple sites of interaction, its dimensions are 8.5 Å in depth and 11.6 Å in width, where, bulky molecules can easily access the major groove. Conversely, the minor groove, which has a depth of 8.2 Å, is narrower and has fewer binding sites, however, binding to the minor groove is the most common. The third mode of interaction is intercalation which is closely related to most anticancer drugs which are currently in clinical use. In essence, small molecules can interact with DNA involving a single or mixed binding mode (Bhaduri et al., 2018). In this paper, our focus will be on DNA intercalation. DNA intercalators are a class of compounds that can reversibly bind to DNA through insertion between adjacent base pairs perpendicularly to the axis of the helix. These

interactions can lead to conformational changes involving an increase in the vertical separation between base pairs, unwinding and lengthening of the DNA helix. It may also interfere with the detection and function of associated proteins or enzymes leading to the failure of DNA repair systems, transcription processes or replication of the DNA (Biebricher *et al.*, 2015). Numerous clinical intercalating agents are available as anticancer agents, for example daunomycin, doxorubicin, mitoxantrone or dactinomycin. Ethidium bromide is a phenanthridine monomer dye frequently used as a fluorescent marker (nucleic acid stain) in molecular biology for many procedures such as visualization of nucleic acid. Ethidium bromide intercalates between adjacent base pairs in the double-stranded DNA molecule and leads to deformation of the DNA. The deformation of DNA will possibly affect DNA biological processes, such as DNA transcription or replication (Binaschi *et al.*, 2001). DNA intercalators have three main structural features: i) Chromophores, which are planar polyaromatic rings that bind to DNA, ii) cationic moieties, such as protonated amino groups which may interact with the phosphate backbone and iii) side chains that can interact with DNA minor grooves. In general, DNA intercalators are classified into two major classes: monofunctional and bifunctional (El-Adl *et al.*, 2020). Monofunctional intercalators also referred to as simple intercalators. They consist of one intercalating unit, often carrying a positive charge on their ring system (Wadler *et al.*, 1994). Secondly, bifunctional intercalators, also called bis-intercalators orthreading intercalation, have two typically cationic intercalating units separated by flexible linker groups being long enough to permit double intercalation. Since bis-intercalators have two different intercalating moieties, they can cause stronger binding with DNA than simple mono-intercalators (Wadler *et al.*, 1994). Schiff bases are ranked among the most privileged synthetic organic intermediates extensively employed in industrial, pharmaceutical, and medical concerns. These compounds are also known as imines or azomethines with a general formula $R-CH=N-R'$, where R and R' are an alkyl or aryl group (Peng *et al.*, 2014). Schiff bases have been reported to exhibit a wide spectrum of biological properties and can also interact with other ligands like *ortho*-phenylenediamines which leads to diverse and multipurpose applications (Koll, 2003). Bis-Schiff bases are usually synthesized from the condensation reaction of diamines with two equivalents of aldehyde or ketone in 1:2 molar ratio. The bases can be either symmetric or asymmetric structures, depending on the reacting aldehydes or ketones. (Vernekar & Sawant, 2023). Literature review revealed a great interest on *ortho*-phenylenediamines Schiff complexes and their applications. In contrast, less attention has been focused on the uncoordinated Schiff bases of *ortho*-phenylenediamines. In this regard, the search for other uncoordinated anticancer agents with improved safety profiles has become an attractive area of study for cancer management (Lucaciu *et al.*, 2022). The main aim of this work is to design and synthesize some symmetrical Schiff's base derivatives of *o*-phenylenediamine and study their DNA intercalating ability using an ethidium bromide competition fluorescent assay and UV-visible spectroscopic method. In addition, there is increasing interest to explore how different structural features of 1, 2-Phenylenediamine Schiff's base derivatives can affect the DNA binding capability using molecular modeling tools, which may serve as a basis for understanding the molecular mechanism of action of the 1, 2-Phenylenediamine Schiff's base derivatives and can help to design new chemotherapeutic molecules.

2. Material and Methods

2.1 Molecular docking

Molecular docking is an *in silico* method for recognizing the correct binding pose of a DNA-ligand complex and evaluating its strength using

various scoring functions for selecting the best pose generated by each molecule to a rank-order. The molecular docking studies of all compounds with DNA were performed using PyRx software to generate grid, calculate dock scores and evaluate conformers. The steps of molecular docking include DNA structure optimization, *in silico* preparation for standard and designed compounds, and process of docking calculations (Adelusi *et al.*, 2022).

2.1.1 Optimization of DNA molecule

The crystal structures of B-DNA fragments (PDB ID: 1BNA, 1D60, 1ZEW, 2DES and 1DCO) were downloaded from the protein data bank (<http://www.rcsb.org/pdb>), and analyzed for its active site by Biovia Discovery Studio Visualizer (<http://accelrys.com>). Auto Dock 4.2 software was used to correct the imported DNA coordinates (The corrections involved deleting unwanted water molecules, adding hydrogen atoms (polar only) followed by adding kolloman charge, and saved as pdpqt format used as input in PyRx software.

2.1.2 Designing and *in silico* preparation of NHM compounds

The starting geometry of all investigated compounds was constructed using Chem3D Ultra (version 12.0, Cambridge soft Com., USA). The optimized geometry of tested compounds with the lowest energy was used in further processes of molecular docking. Discovery studio visualizer was used to all tested compounds in which the compounds were converted to PDB files that will be used as input in PyRx software.

2.1.3 Docking process and analysis

B-DNA crystal structures (PDB ID: 1BNA, 1D60, 1ZEW, 2DES and 1DCO) were loaded in PyRx virtual screening tools as pdbqt format. Standard drug and designed compounds pdb files were loaded and automatically converted to pdbqt format. Docking was performed using Autodock Vina incorporated in Pyrx software. The centers of the grid box were assigned automatically and the dimensions of the box were set to $25 \times 25 \times 25 \text{ \AA}$. After docking, the complexes with the lowest binding energy (kcal/mol) were selected and their interaction modes were visualized by Discovery Studio.

2.2 Prediction of ADMET properties and drug-likeness

The *in silico* procedure has become a very important tool in drug identification and screening. Ligand absorption, distribution, metabolism and excretion (ADME) pharmacokinetic properties of the designed Schiff's base derivatives of *o*-phenylenediamine, are evaluated to determine their activity within the human body and prediction of these properties in advance will save the cost of drug discovery substantially. To verify drug-likeness, canonical SMILES format of the designed NHM compounds were used in swissADME (<http://www.swissadme.ch/index.php>). The main bioavailability parameters were molecular weight (g/mol), lipophilicity (XlogP3), solubility (log S), polarity (Topological Polar Surface Area - TPSA in \AA^2), saturation (fraction of carbon atoms in Sp3 hybridization - Csp3) and flexibility (No of rotatable bonds). Consequently, absorption parameters such as Human Intestinal Absorption, Blood Brain Barrier, P-glycoprotein interaction (substrate or inhibitor) and metabolism (inhibitor or substrate) of the bio-active molecules with different cytochrome P450 enzymes were also estimated using admetSAR, which is based on QSAR data for prediction of absorption, distribution, metabolism, excretion and toxicity (ADMET). Drug-like molecules considering Lipinski rules and good ADMET properties were chosen as ligands in consequent molecular docking procedure.

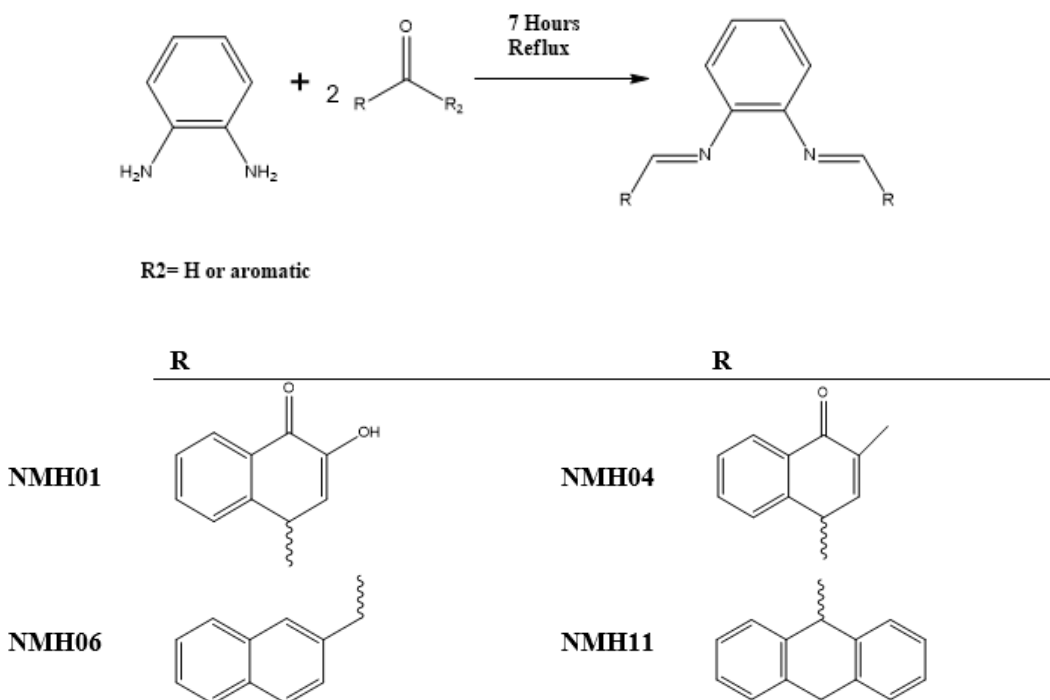
2.2.1 SwissADME

Swiss ADME is a free web tool developed by the Swiss Institute of Bioinformatics (SIB), it was employed to evaluate pharmacokinetics, drug-likeness and medicinal chemistry friendliness of small molecules and freely available at www.swissadme.ch. It calculates six physicochemical properties: lipophilicity, size, polarity, solubility, flexibility, and saturation. In addition, it promotes the assessment of ADME parameters (absorption, distribution, metabolism and excretion) of drug candidates and molecules and provides information to determine Lipinski's rule of five for drug likeness of oral bioavailability (Daina *et al.*, 2017). The drug-likeness assessment is based on the following factors: molar mass smaller amount than 500 g mol⁻¹, 1 Log P is a smaller amount than five, number of acceptors of hydrogen bonds is a smaller amount than 10; accounted for in the molecule function of N or O atoms, and number of donors of hydrogen bonds is a smaller amount than 5, accounted for in the molecule function of NH or OH groups. Hence, the molecules outside this range will be unlikely to become orally bioavailable as a drug (Lipinski *et al.*, 2001).

2.3 Chemistry

2.3.1 General procedure for Synthesis of Schiff base (NHM Compounds):

Schiff's bases were prepared by reacting of one mole of phenylenediamine and two moles of substituted aromatic aldehydes or ketones in 100 ml ethanol. The solution was refluxed for 7hrs under constant stirring. The condensation reaction was carried out by using glacial acetic acid as a catalyst and monitored by thin layer chromatography (TLC). The mixture was left for cooling and the solid product (crude) was gathered by filtration and washed four times with ethanol and then dried utilizing vacuum. The gained product was re-dissolved in ethanol for recrystallization and after that dried to give a clean pure product (**Scheme 1**). The crystalline products obtained were characterized by Fourier-Transform Infrared (FTIR) spectra (Cary 600 FTIR, USA), which was operated in wavenumber range of 4000–400 cm⁻¹, and ¹H and ¹³C nuclear magnetic resonance (NMR) spectroscopies were performed with *dimethyl disulfide* (DMDS) used as solvent. Tetramethylsilane (TMS) was the standard reference, and the probe temperature was 25°C (Hamil *et al.*, 2009).



Scheme 1: General scheme for the synthesis of Schiff base NHM Compounds.

((4Z,4'E)-4,4'-(1, 2-phenylenebis (azanylylidene)bis (2-hydroxynaphthalene-1(4H)-one) (NHM01)

NMH01 has been synthesized according to the general procedure, by reacting of one mole of phenylenediamine and two moles of 2-hydroxynaphthalene-1,4-dione in 100 ml ethanol.

Spectral data

Orange crystals, mp 240-241°C, yield: 62%; %; FTIR (cm⁻¹):3570 (O-H), 1619(C=O) 1586(C=N), 1445(C-N),1216(C-O). ¹H NMR (400 MHz, DMSO-d₆, δ ppm) 7.84-8.29(m, 12H, C-H aromatic), 7.19 (s, 1H, C-H aromatic), 15(s, 2H, OH). ¹³CNMR (400 MHz, DMSO-d₆):189.10, 157.04, 145.42, 142.65, 139.36, 139.62, 131.07, 130.29,130.16, 129.38,

128.84, 128.60, 128.23, 124.90, 123.00,103.00 .Anal Calcd for C₂₆H₁₆N₂O₄: C, 74.28; H, /3.84; N, 6.66; O, 15.22.

(4Z,4'Z)-4,4'-(1,2-phenylenebis (azanylylidene) bis(2-methylnaphthalene-1(4H)-one)NHM04compound:

NMH04 has been synthesized according to the general procedure, by reacting of one mole of phenylenediamine and two moles of 2-methylnaphthalene-1,4-dione in 100 ml ethanol.

Spectral data

Green crystals, mp 241-242°C, yield: 75%; FTIR (cm⁻¹):3053 (C-H, Aromatic), 2965 C-H (CH₃)3570 (O-H), 1600(C=O) 1550(C=N), 1526

(C=C), 1440(C=N), 1220(C-O). ¹H NMR (400 MHz, DMSO-d₆, δ ppm) 7.30-8.05 (m, 12H, C-H aromatic), 6.9 (s, 1H, CH=C aromatic), 2.09 (s, 6H, CH₃). ¹³C NMR (400 MHz, DMSO-d₆); 184.81, 147.82, 135.02, 133.77, 133.74, 131.59, 131.56, 125.82, 125.13, 16.50. Anal Calcd for C₂₈H₂₀N₂O₂: C, 80.75; H, 4.84; N, 6.73; O, 7.68.

(*N*¹*E*,*N*²*E*)-*N*¹,*N*²-bis (naphthalen-1-ylmethylene)benzene-1,2-diamine) NHM06 compound:

NMH06 has been synthesized according to the general procedure, by reacting of one mole of phenylenediamine and two moles of 1-naphthaldehyde in 100 ml ethanol.

Spectral data

White crystals, mp 239-240°C, yield: 65%; FTIR (cm⁻¹): 3045(C-H aromatic), 1529(C=N), 1446(C=C), 1397(C-N) ¹H NMR (400 MHz, DMSO-d₆, δ ppm): 7.32-8.05 (m, 18H, C-H aromatics), 9.1 (s, 2H, CH=N). ¹³C NMR (400 MHz, DMSO-d₆); 156.00, 140.41, 135.18, 134.84, 133.42, 133.36, 130.42, 130.31, 127.88, 127.68, 126.63, 124.13, 116.39. Anal Calcd for C₂₈H₂₀N₂: C, 87.47; H, 5.24; N, 7.29.

(*N*¹,*N*²-di(anthracen-9(10H)-ylidene)benzene-1,2-diamine) NMH11 compound:

NMH11 has been synthesized by the described procedure, by reacting of one mole of phenylenediamine and two moles of anthracen-9(10H)-one in 100 ml ethanol.

Spectral data

Light green crystals, mp 291-292°C, yield: 80%; FTIR (cm⁻¹): 3287(C-H aromatic), 3060(C-H SP₃), 1655 (C=N), 1577(C=C), 1308(C-N). ¹H NMR (400 MHz, DMSO-d₆, δ ppm) 3.81 (s, 4H, CH₂), 7.30-7.72 (m, 20H, C-H aromatics). ¹³C NMR (400 MHz, DMSO-d₆); 185.01, 148.62, 140.85, 139.86, 134.35, 132.81, 131.94, 128.91, 127.68, 127.59, 126.55, 125.37, 125.34, 123.44, 122.35 119.74, 116.43, 50.01. Anal Calcd for C₃₄H₂₄N₂: C, 88.67; H, 5.25; N, 6.08.

2.4 DNA binding studies

To study how competently the synthesized compounds interact with G-DNA, the synthesized compounds were investigated for their DNA binding ability using fluorescence emission spectra. All experiments were conducted in *Tris* (Hydroxymethyl)aminomethane (*Tris* buffer) (0.01M *Tris*, 0.1M NaCl, at pH 7.4), glass-distilled deionized water and analytical grade reagents were used throughout experiments. The pH values of all solutions were measured with a calibrated Jenway pH-meter model 3510 (Staffordshire, UK). All buffer solutions were filtered through Millipore filters (Millipore, UK) of 0.45 mm pore diameter.

2.4.1 Absorbance spectra

Absorbance spectra were measured on a Jenway UV-visible spectrophotometer, model 6505 (London, UK) using quartz cells of 1.00cm path length. The UV-Vis absorbance spectra were recorded in the 200-500nm range, and spectral bandwidth of 3.0nm. For the final spectrum of each solution analyzed baseline subtraction of the buffer solution was performed. Genomic DNA was used in a concentration of

75 µg/ml. DNA was extracted from peripheral lymphocytes of anticoagulated blood (EDTA) samples by Proteinase K digestion and phenol/chloroform extraction. Purity was determined by measuring the absorbance at 260/280nm indicating that the sample is free from protein contamination. The concentration was assayed spectrophotometrically using 6600M⁻¹cm⁻¹ as a molar extinction coefficient at 260nm.

2.4.2 Fluorescence spectra and DNA-binding studies

Fluorescence emission and excitation spectra were measured using a Jasco FP-6200 spectrofluorometer (Tokyo, Japan) using fluorescence 4-sided quartz *cuvettes* of 1.00 cm path length. The automatic shutter-on function was used to minimize photo bleaching of the sample. The selected excitation wavelength for ethidium bromide was 480nm. The emission spectrum was corrected for background fluorescence of the buffer. The ethidium bromide (EB) fluorescence displacement experiment was performed by sequential addition of aliquots of 1790 µl *Tris* buffer, 10 µl EB (final concentration of 72µM), 100µl G-DNA from stock solutions (1.5 mg/ml) and finally 10 µl of compounds (NHM compounds, final concentration of 30 µM). Emission spectra were recorded for each system using excitation wavelengths of maximum fluorescence intensity determined for the systems to be 480nm using a slit width of 5nm to examine alterations in emission spectra resulting from the complex construction of both systems. On construction of the full systems, the system was allowed to equilibrate for 30minutes at room a temperature and emission spectra (500-730nm) were recorded to monitor changes in EB intensity.

3 Results and Discussion

3.1 Design strategy of *ortho*-phenylenediamine Schiff's base derivatives

Based on the increased role and importance of phenylenediamine Schiff's base derivatives as DNA intercalators as described in the introduction part, and because of their versatile route of chemical synthesis, *ortho*-phenylenediamine were used as key scaffold to develop a series of aromatic imino analogues. Fifteen compounds named with NHM symbol were designed, the strategy which applied to design these compounds was based on the symmetrical distribution of the amino groups of *ortho*-phenylenediamine with different carbonyl compounds including naphthaldehyde, naphthoquinone and anthraquinone derivatives, where the aldehydes or ketones differ in their lipophilicity, hydrogen bond ability as donor or acceptors, and ionizability. The applied strategy yielded the scaffold which contains three parts: 1) A planar polycyclic pattern to intercalate between DNA base-pairs and to provide π-π interactions. 2) Some polar functions providing hydrogen bond interactions with nucleic acids. 3) Variety of substituents to improve the interactions and promote the physicochemical properties. To the best of our knowledge, there have been no literature reports regarding Schiff's base of *ortho*-phenylenediamine with *naphthoquinones* and anthraquinone derivatives as DNA intercalating agent so far. The designed compounds were investigated for their docking energies. In addition, the effect of replacing of the naphthyl ring with a three ring system (anthracene) or aromatic rings with flexible linkage was also investigated. The chemical structures are listed in Table 1.

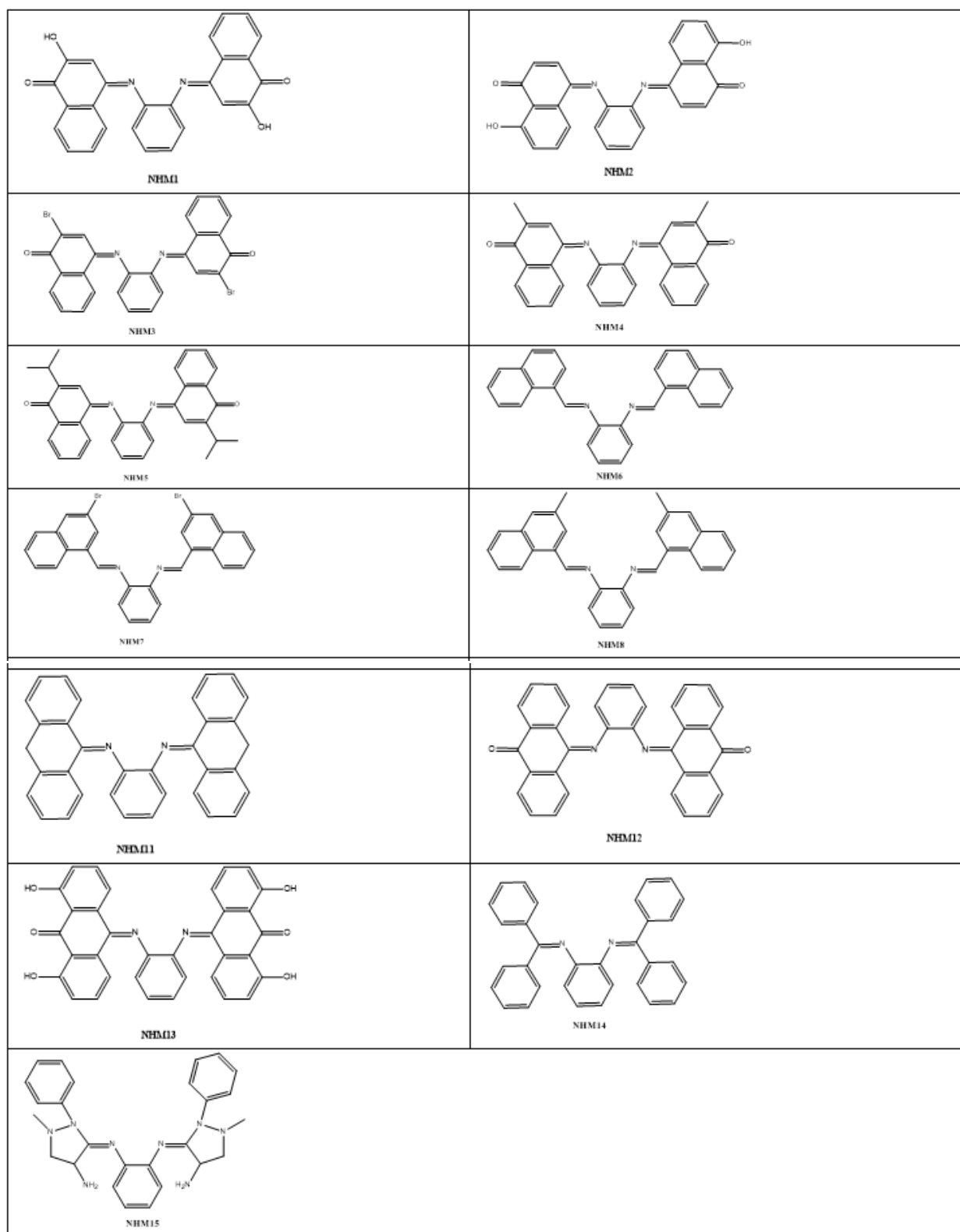


Table 1: The chemical structures of designed compound

3.2. Molecular docking analysis

In this part of the current study, the molecular dockings of NHM compounds with five B-DNA fragments were performed using Auto Dock vina in PyRx Virtual Screening Tool to understand the possible

binding mode. The molecular docking study was employed to identify the binding interactions and estimate the binding affinity of the most active derivatives to the DNA duplex by combining and optimizing variables such as hydrophobic, steric, and electrostatic complementation. Two

well-known biologically active DNA intercalating agents were used as references namely doxorubicin and daunorubicin. Considering the values of free energies of binding mentioned in Table 2, it could be deduced that the compounds were properly accommodated between the DNA base

pairs. The molecular docking analysis revealed that the compounds have contributed in hydrophobic and *Pi-Pi* interactions, and hydrogen bonding with the DNA base pairs.

Names of compound	Docking Energy(kcal/mol)				
	1D60	1ZEW	2DES	1BNA	1DC0
Daunorubicin	-8.9	-10.0	-8.8	-8.9	-9.8
Doxorubicin	-8.6	-9.8	-8.4	-8.8	-9.6
NHM01	-9.2	-10.9	-9.1	-8.9	-8.8
NHM02	-7.7	-9.4	-9.1	-8.6	-8.8
NHM03	-6.8	-8.5	-8.4	-7.3	-8.1
NHM04	-7.3	-8.1	-8.7	-6.9	-8.0
NHM05	-6.9	-8.2	-9.7	-6.5	-8.0
NHM06	-7.3	-8.1	-7.7	-8.1	-7.2
NHM07	-7.3	-8.3	-8.0	-7.3	-7.2
NHM08	-7.0	-8.6	-9.0	-7.5	-7.3
NHM09	-8.6	-8.3	-8.6	-8.1	-7.3
NMH10	-7.2	-7.8	-7.6	-7.7	-7.6
NMH11	-8.9	-9.1	-8.4	-8.4	-8.5
NMH12	-8.3	-9.4	-9.3	-8.5	-8.8
NMH13	-8.9	-9.0	-9.4	-8.5	-8.8
NMH14	-6.5	-7.2	-6.4	-6.3	-7.1
NMH15	-6.0	-7.2	-6.3	-6.7	-7.4

Table 2: Various energies in the binding process of NHM compounds with DNAs obtained from molecular docking.

(1BNA): D(CGCGAATTCGCG)², (1DC0): D(CATGGGCCCATG)², ((2DES): D(CGTACG)², (1D60) :D(CCAACNTTGG)², (1ZEW): D(CCTCTAGAGG)²,

ΔG^a is the binding free energy change in the binding process.

The more negative the numerical values for the binding affinity, the better is the predicted binding between a ligand and a macromolecule. In this particular case of screening five DNA fragments (1BNA, 1ZEW, 2DES, 1D60, 1BNA and 1DC0) with designed compounds. Table 2 shows that all the designed compounds have good binding energies when compared to standard drugs. Moreover, NMH01 and NMH11 are both predicted to have the best binding affinity.

The DNA fragment (1zew) was used to discuss and compare the intercalating activity of all compounds. It appears worth to note that compounds which exhibit high activity against (1zew) also showed high activity against the other DNA fragments. Simultaneously, any modification which might decrease the activity against (1zew) will produce the same effect against all other DNA fragments.

Molecular docking results were identified based on the strongest ligand binding poses, where identified using the low binding energy and the number of H-bonding and hydrophobic interactions. From the docking studies the molecular docking analysis revealed that all the docked molecules were inserted between the adjacent nucleotides at the active site. These compounds were stabilized at the active site through different interactions. The planar system was involved in hydrophobic stacking with the base pairs of different nucleotides, and the hydrophilic moieties formed several hydrogen bonds with different nucleotides.

It was observed that introduction of hydrophilic substituent's to the aromatic ring increases the intercalating activity (decrease of the docking energy) as shown with NMH01, NMH09 and NMH13. While, the introduction of hydrophobic substituents (R) to the same aromatic ring leads to a decrease of the intercalating activity (increase of the docking

energy) as shown for NMH04 and NMH08. A substantial observation was that the highest activity was predicted to be with an introduction of 2-hydroxynaphthalene-1,4-dione at NMH01. The importance of hydroxyl substituents at *meta*-positions of the aromatic ring are attributed to the formation of seven hydrogen bonds at intercalating sites keeping the planarity which is needed for optimum localization at the intercalating site (**Figure1**). Whereas, hydroxyl substituent at position five builds three H-bonds as shown in NMH02. H-bonding characteristics of compounds rendered significantly high binding affinity with DNA.

Lipophilic substituents (Cl or Br) at position 3 of the naphthyl side chain had little effect on the intercalating activity when compared with the non-substituted derivative (NMH03, NMH07). Furthermore, introduction of a hydrogen bond acceptor substituent such as carbonyl group on the aromatic ring leads to an increase of the intercalating activity, as could be seen from the comparison of 2-hydroxynaphthalene-1,4-dione derivatives with the corresponding non-substituted 2-hydroxynaphthalene derivatives as shown with NMH01, NMH02 and NMH09. In the case of compounds NMH04, NMH08, NMH05 and NMH10 replacement of the methyl moiety on aromatic rings with the isopropyl moiety leads to a decrease of the intercalating activity, which may be caused by steric hindrance of branched groups. Furthermore, as observed in the docking study, compound NMH14 was located at the groove pocket interacting with DNA by *pi*-anion interaction with DGB:17 and DGA:7. Compound NMH15 was located at the groove pocket and interacted with DNA by six hydrogen bonds with DGA:10, DGA:9, DTB:15 and DAB:16. Nevertheless, it was evident that NMH14 and NMH15 had the lowest binding energy scores which may be due to the lack of the planarity pattern of the polyaromatic systems.

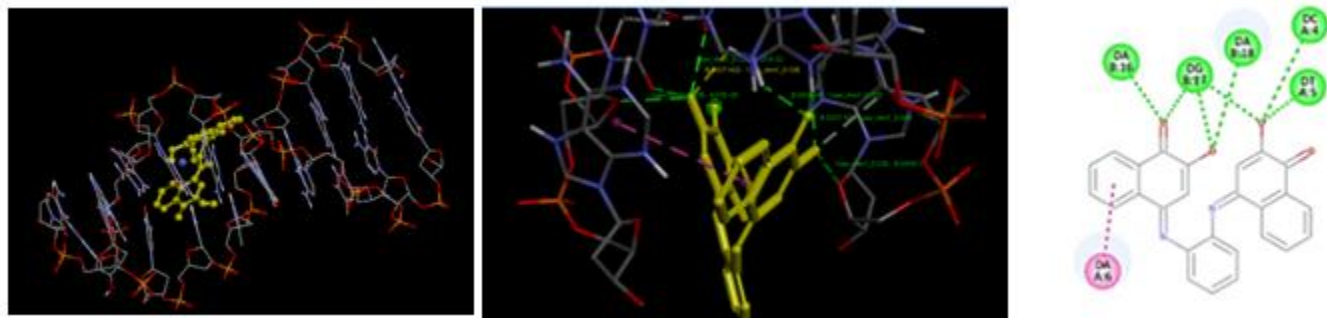


Figure 1: Localization of NHM01 (yellow) at the intercalating site of DNA. (ii) Compound NMH01 interacting with DNA strands with seven intermolecular hydrogen bonds. (iii) 2-dimensional structure of NMH01 at the active site.

It can be clearly seen that the interaction mode of most compounds consist of a classical intercalation mode except the binding of NMH03, NMH05, NMH08 and NMH10 with DNA which involves partial intercalation and groove binding. Moreover, compounds NMH14 and NMH15 bind to DNA *via* groove binding. It is worth mentioning that compounds NMH01, NMH04, NMH06 and NMH11 were the most active compounds for each DNA fragment (Table 2). For this reason they have been selected for further synthesis and analysis.

3.3 ADMET properties

3.3.1 Analysis of Physicochemical Properties.

General characteristics of designed Schiff's base derivatives of *o*-phenylenediamine revealed that all these compounds have a molecular weight less than 500 g/mol, except NMH03, NMH07, and NMH13 with molecular weights of 546.21, 542.26 and 552.53g/mol, respectively. This appears a prime property to be called as drug likeness of the small

molecules. It is evident from Table 3 topological polar surface area (TPSA) values of all compounds were found to be within the limit of $\leq 140 \text{ \AA}$. The prediction of TPSA parameters helps to understand the passive molecular transport of drug molecules. TPSA is an important tool in drug discovery and development. By analyzing a drug candidate's TPSA, we can predict its potential for oral bioavailability and ability to reach target sites within the body. This prediction hinges on a drug's ability to permeate biological barriers. The Molar refractivity (MR) of all compounds is within the ranges of 121.50–158.01, their number of rotatable bond (nRotb), number of H-bond donors (nHBD) and the number of hydrogen bond acceptors (NHBA) of all *o*-phenylenediamine derivatives are within the recognized limits ≤ 10 , ≤ 5 , and ≤ 10 , respectively.

SwissADME predictions suggest that symmetrical phenylenediamine Schiff's base derivatives have optimum parameters for anticancer activity and can be considered as lead molecules for further modifications.

Compound	MW (g/mol)	nHA	nRB	nHBD	nHBA	MR	TPSA (Å ²)
NHM01	420.42 g/mol	32	2	2	6	121.80	99.32Å ²
NHM02	420.42 g/mol	32	2	2	6	122.71	99.32Å ²
NHM03	546.21 g/mol	32	2	0	4	134.40	58.86Å ²
NHM04	416.47 g/mol	32	2	0	4	128.27	58.86Å ²
NHM05	472.58 g/mol	36	4	0	4	147.50	58.86 Å ²
NHM06	384.47 g/mol	30	4	0	2	128.85	24.72Å ²
NHM07	542.26 g/mol	32	4	0	2	144.25	24.72Å ²
NHM08	412.52 g/mol	32	4	0	2	138.78	24.72Å ²
NHM09	416.47 g/mol	26	4	2	4	132.89	65.18Å ²
NMH10	468.63 g/mol	36	6	0	2	158.01	24.72Å ²
NMH11	460.57 g/mol	36	2	0	2	148.83	24.72Å ²
NMH12	488.53 g/mol	38	2	0	4	149.67	58.86Å ²
NMH13	552.53 g/mol	42	2	4	8	157.76	139.78Å ²
NMH14	436.55 g/mol	34	6	0	2	142.81	24.72Å ²

NMH15	454.57 g/mol	34	4	2	6	152.22	89.72Å ²
-------	-----------------	----	---	---	---	--------	---------------------

Table 3: Physicochemical properties of designed Schiff's base derivatives of *o*-phenylenediamine calculated using swissADME database.

Molecular weight: M. W, Number of heavy atom: nHA, , Number of rotatable bonds: nRB, Number of H-bond acceptors: nHBA, Number of H-bond donors: nHBD, Molar refractivity: MR, topological polar surface area: TPSA.

3.3.2 Lipophilicity and Water Solubility.

Log Po/w values of all derivatives range from 2.85 to 8.00 reflecting its partition preferably into the lipid compartment (Table 4). This implies that

these compounds will be well absorbed through the membranes into the systemic circulation to achieve high bioavailability. On the other hand, solubility, Log Sis aqueous solubility, exhibit a defined range of -4.4to-8.72 as shown in Table 5. The compounds NMH01, NMH02, NMH03, NMH15 predicted as moderately soluble (with optimal lipophilicity and moderate water solubility) can achieve good bioavailability when administered orally. All other derivatives are poorly water soluble.

Compound	iLOGP	XLOGP3	WLOGP	MLOGP	SILICOS-IT	Consensus Log Po/w
NHM01	2.62	4.36	5.20	1.25	5.06	3.70
NHM02	3.15	5.04	4.84	1.79	5.10	3.98
NHM03	3.20	6.45	6.88	3.49	7.37	5.48
NHM05	4.13	6.92	7.49	4.06	8.35	6.19
NHM06	4.13	7.02	7.49	5.35	7.89	6.38
NHM07	4.09	8.40	9.02	6.46	9.22	7.44
NHM08	4.04	7.75	8.11	5.74	8.94	6.92
NHM09	3.57	6.31	6.91	4.15	6.91	5.57
NMH10	4.32	9.27	9.74	6.48	10.21	8.20
NMH11	4.26	8.46	7.83	6.03	9.19	7.15
NMH12	3.62	7.49	7.11	4.17	8.56	6.19
NMH13	3.88	7.17	5.91	2.01	6.63	5.13
NMH14	3.89	8.28	8.02	6.05	8.40	6.93
NMH15	3.62	2.58	1.61	3.73	1.08	2.52

Table 4: The lipophilicity of designed Schiff's base derivatives of *o*-phenylenediamine calculated with SwissADME database.

Compound	ESOL		Ali		SILICOS- IT	
	Log S (ESOL)	Class	Log S (Ali)	Class	Log S SILICOS-IT	Class
NHM01	-5.48	Moderately soluble	-6.16	Poorly soluble	-7.75	Poorly soluble
NHM02	-5.91	Moderately soluble	-6.87	Poorly soluble	-7.31	Poorly soluble
NHM03	-7.57	Poorly soluble	-7.48	Poorly soluble	-10.47	Insoluble
NHM04	-6.11	Poorly soluble	-6.39	Poorly soluble	-9.68	Poorly soluble
NHM05	-7.24	Poorly soluble	-7.97	Poorly soluble	-10.49	Inoluble
NHM06	-7.02	Poorly soluble	-7.35	Poorly soluble	-10.90	Insoluble
NHM07	-8.83	Poorly soluble	-8.79	Poorly soluble	-12.44	Insoluble
NHM08	-7.62	Poorly soluble	-8.11	Poorly soluble	-11.65	Insoluble
NHM09	-6.73	Poorly soluble	-7.47	Poorly soluble	-9.73	Poorly soluble
NMH10	-8.72	Poorly soluble	-9.69	Poorly soluble	-12.47	Insoluble
NMH11	-8.51	Poorly soluble	-8.85	Poorly soluble	-13.50	Insoluble
NMH12	-8.04	Poorly soluble	-8.56	Poorly soluble	-13.24	Insoluble
NMH13	-8.18	Poorly soluble	-9.93	Poorly soluble	-10.87	Insoluble
NMH14	-8.02	Poorly soluble	-8.66	Poorly soluble	-12.54	Insoluble
NMH15	-4.41	Moderately soluble	-4.41	Moderately soluble	-5.97	Moderately soluble

Table 5: Water solubility characteristics of designed Schiff's base derivatives of *o*-phenylenediamine calculated with swissADME database

3.3.3 Pharmacokinetic Profile

Values of ADME properties of designed *o*-phenylenediamine derivatives presented in Table 6 were all within the permissible range. All of the compounds have a low gastro intestinal absorption except NMH01, NMH02, NMH04 and NMH15 show high gastrointestinal absorption. All these compounds lack blood brain barrier (BBB) penetration. BBB is very important to limit the penetration of drugs into the central nervous system

(CNS). The lack of BBB penetration ability suggests their low CNS side effects as well as their unsuitability to treat brain tumors'. In the present study, all the compounds were predicted to be non-substrate of *P*-glycoprotein, except compounds NMH06, NMH07, NMH08, NMH09, NMH10, NMH14 and NMH15. In the case of drug metabolism NMH01 was identified as an inhibitor of CYP1A2, CYP2C9 and CYP3A4. Compound NMH04 was predicted as an inhibitor of CYP2C9, CYP2C19 and CYP3A4 and in addition, NMH06 as CYP1A2, CYP2C19 and

CYP3A4 inhibitors. However, NMH11 was predicted to show no inhibitory activity against any of the CYP isoforms. The skin permeability coefficient (Log Kp, a multiple linear regression, Potts and Guy, 1992), indicates the more negative the log Kp (with Kpin cm/s), the less skin

permeant is the molecule. Among the NHM compounds, NMH15 (-7.24 cm/s) is the least permeant compound and NMH10 (-2.58 cm/s) is most permeant, respectively.

Compound	Absorption	BBB Permeant	P-gp substrate	CYP1A2 inhibitor	CYP2C19 inhibitor	CYP2C9 inhibitor	CYP2D6 inhibitor	CYP3A4 inhibitor	Log Kp (Skin Permeation) (cm/s)
NHM01	High	No	No	Yes	No	Yes	No	Yes	-5.77 cm/s
NHM02	High	No	No	Yes	Yes	Yes	No	Yes	-5.29 cm/s
NHM03	Low	No	No	No	No	Yes	No	No	-5.05 cm/s
NHM04	High	No	No	No	Yes	Yes	No	Yes	-5.01 cm/s
NHM05	Low	No	No	No	No	No	No	Yes	-4.27 cm/s
NHM06	Low	No	Yes	Yes	Yes	No	No	Yes	-3.66 cm/s
NHM07	Low	No	Yes	Yes	No	No	No	No	-3.64 cm/s
NHM08	Low	No	Yes	Yes	No	No	No	Yes	-3.31 cm/s
NHM09	Low	No	Yes	Yes	Yes	No	No	No	-4.36 cm/s
NMH10	Low	No	Yes	No	No	No	Yes	Yes	-2.58 cm/s
NMH11	Low	No	No	No	No	No	No	No	-3.10 cm/s
NMH12	Low	No	No	Yes	No	No	No	No	-3.96 cm/s
NMH13	Low	No	No	No	No	No	No	No	-4.58 cm/s
NMH14	Low	No	Yes	Yes	Yes	No	No	Yes	-3.08 cm/s
NMH15	High	No	Yes	No	No	No	Yes	No	-7.24 cm/s

Table 6: Pharmacokinetic parameters of designed Schiff's base derivatives of *o*-phenylenediamine calculated with swissADME database.

3.3.4 Drug likeness

NMH01 do not violate any of the five drug likeness parameters, *i.e.*, Lipinski, Muegge, Ghose, Veber, and Eganrules of drug likeness(Daina *et al.*, 2017). The other compounds showed violation of at least one of the drug-likeness filters. As per Lipinski's rule-of-five, candidates violating none or less than one of the following four criteria are likely to be developed as a prospective oral drug. The criteria are as follows: log P (octanol-water partition coefficient) ≤ 5 , molecular weight ≤ 500 , number of hydrogen bond acceptors ≤ 10 and number of hydrogen bond donors ≤ 5 . In this investigation, none of the designed Schiff's base derivatives of *o*-phenylenediamine compounds has violated Lipinski's rule of five except NMH07 which has two violations: MW>500 and MLOGP>4.15 (Table 7) thus providing the possible utility of as eries for developing

compounds with drug-like properties. All derivatives have a similar bioavailability score of 0.55. The results obtained from *in silico* studies using SwissADME clearly indicate that the selected compounds to be synthesized, namely NMH01, NMH04, NMH06 and NMH11 could be druggable substances. It is interesting to note that the results from the SwissADME predictor values of MW1, log P, HBA, HBD, molar refractivity and the total polar surface area of these molecules are in excellent agreement with the most important rules of drug likeness. The results show that all four compounds have zero violations of Lipinski's rule of five. SwissADME predictions suggest that symmetrical phenylenediamine Schiff's base derivatives have optimum parameters for anticancer activity and can be considered as lead molecules for further modifications.

Compound	Lipinski	Hose	Veber	Egan	Muegge	BA. Score
NHM01	Yes	Yes	Yes	Yes	Yes	0.55
NHM02	Yes	Yes	Yes	Yes	No;1violation: XLOGP3>5	0.55
NHM03	Yes;1violation: MW>500	No; 3 violations: MW>480,WLOGP>5.6, MR>130	Yes	No;1violation: WLOGP>5.88	No;1violation: XLOGP3>5	0.55
NHM04	Yes	No;1violation: WLOGP>5.6	Yes	No;1violation: WLOGP>5.88	No;1violation: XLOGP3>5	0.55
NHM05	Yes	No; 2 violations: WLOGP>5.6,MR>130	Yes	No; 1 violation: WLOGP>5.88	No;1violation: XLOGP3>5	0.55
NHM06	Yes;1violation: MLOGP>4.15	Yes	No;1violation: WLOGP >5.88	No;1violation: WLOGP>5.88	No;1violation: XLOGP3>5	0.55
NHM07	No;2violations: MW>500,MLOGP>4.15	No;3violations: MW>480,WLOGP>5.6, MR>130	Yes	No;1violation: WLOGP>5.88	No;1violation: XLOGP3>5	0.17
NHM08	Yes; 1 violation: MLOGP>4.15	No; 2 violations: WLOGP>5.6,MR>130	Yes	No;1violation: WLOGP>5.88	No;1violation: XLOGP3>5	0.55
NHM09	Yes;1violation: MLOGP>4.15	No;2violations: WLOGP>5.6,MR>130	Yes	No;1violation: WLOGP>5.88	No;1violation: XLOGP3>5	0.55

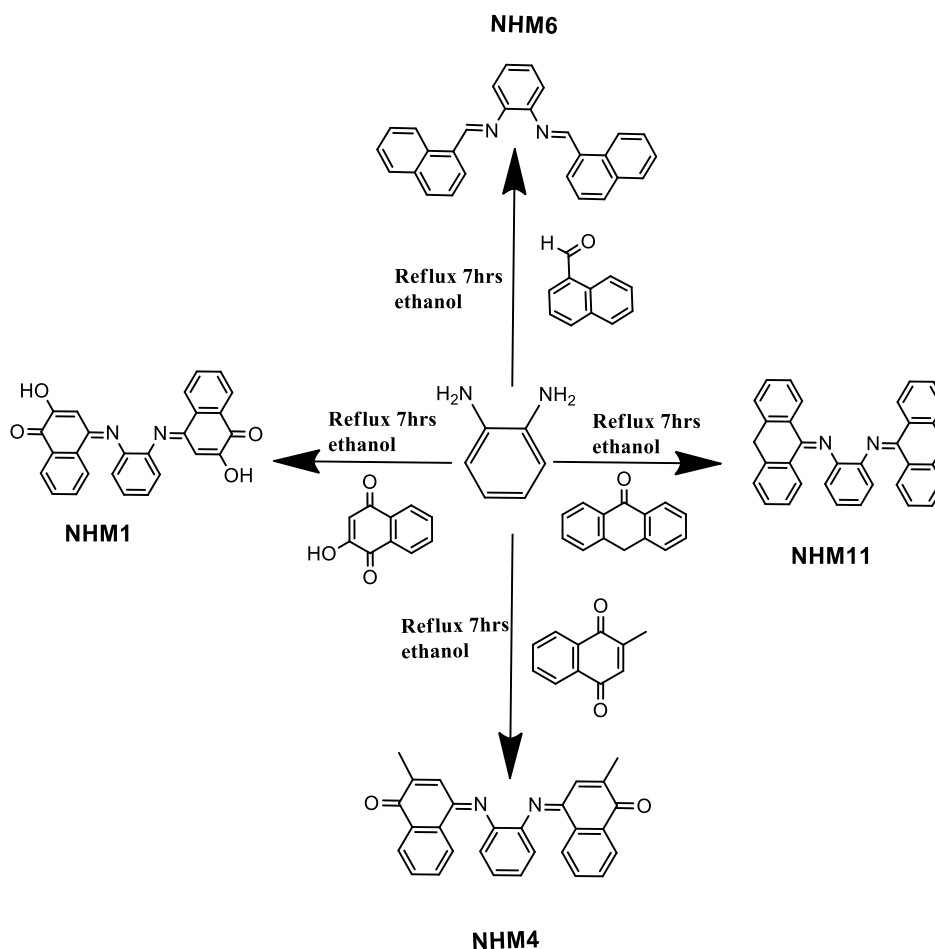
NMH10	Yes;1violation: MLOGP>4.15	No;2violations: WLOGP>5.6,MR>130	Yes	No;1violation: WLOGP>5.88	No;1violation: XLOGP3>5	0.55
NMH11	Yes;1violation: MLOGP>4.15	No;2violations: WLOGP>5.6,MR>130	Yes	No;1violation: WLOGP>5.88	No;1violation: XLOGP3>5	0.55
NMH12	Yes;1violation: MLOGP>4.15	No;3violations: MW>480,WLOGP>5.6, MR>130	Yes	No;1violation: WLOGP>5.88	No;1violation: XLOGP3>5	0.55
NMH13	Yes;1violation: MW>500	No;3violations: MW>480,WLOGP>5.6, MR>130	Yes	No;2violations: WLOGP>5.88,T PSA>131.6	No;1violation: XLOGP3>5	0.55

Table 7: Druglikenessof designed Schiff's base derivatives of *o*-phenylenediamine calculated with swissADME database

3.4 Chemical synthesis

The best four promising compounds according to the *in silico* studies were synthesized. The targeted compounds, symmetrical 1, 2-phenylenediamine with di-substituted aromatic carbonyl moiety, have been successfully synthesized using a previously reported synthetic procedure. The reaction order for the synthesis of selected compounds is

given in general schemes 2. All the derivatives were synthesized producing good yields with characteristic color. The compounds were soluble in chloroform and dimethyl sulfoxide (*DMSO*) but insoluble in water. Melting points were in the range of 239–292 °C. Thin-layer chromatography (TLC) was used to monitor the progress of the reaction in methanol: dichloromethane (1:4). Their chemical structures were confirmed by means of spectroscopic analysis as described previously.



Scheme 2: Synthesis scheme of NHM compounds

Analysis of spectra

Proton ¹H and Carbon ¹³C NMR spectra

NMR analysis is very important to confirm the structure and functional groups. Experimental H-NMR chemical shifts were expressed in ppm,

dispersed through the spectrum starting from tetramethylsilane as the internal standard and recorded in *DMSO-d*. Importantly, the spectra lacked the signal of the amino group (NH) characteristic of the starting material. The ¹H-NMR spectrum of NHM01 displayed singlet at 15 ppm and multiplet at 7.84-8.29 ppm as signal to the O-H proton and the protons

of aromatic rings, respectively. Moreover, a peak appears at 2.09 ppm attributed to the aliphatic-CH (6H) compound contained in NHM04 and multiplet signals at 7.30-8.05 ppm were ascribed to aromatic protons. Besides, the signal due to -CH=N appears at 9.1 ppm for the compound NHM06 corresponding to the azomethine group which confirms the formation of Schiff bases and the multiple peaks attributed to the aromatic protons between 7.32 and 8.05 ppm. Additionally, the $^1\text{H-NMR}$ spectrum of compound NMH11 exhibited as singlet signal at 3.81 ppm corresponding to the CH_2 group. The multiplet signals at 7.30-7.72 ppm were assigned to the 20 H aromatic protons. Consistently $^{13}\text{C-NMR}$ spectra showed a chemical shift at 189.10, 184.81, 156.40, 185.01 ppm assigned to the imine group revealing the formation of Schiff's base derivatives of *o*-phenylenediamine (NHM01, NHM04, NHM06 and NMH11), respectively. In addition, the peak observed at 16.50 ppm was attributed to a methyl carbon (C20) integrated at the aromatic group of compound NHM04. The peaks observed at 157.04 ppm and 183.00 ppm corresponding to carbonyl groups of the compounds NMH01 and NHM04, respectively. The peak at 50.01 ppm attributes to the methylene group of compound NMH11. The peaks at 103.11-148.62 ppm range are ascribed to aromatic carbons.

Fourier-Transformed Infrared

In order to continue the characterization of NHM compounds, the FT-IR spectrum was carried out. The FT-IR spectra of NHM compounds showed the disappearance of both carbonyl groups at the aldehyde, keton or amino groups at the amine, whereas NH is vanished or hidden underneath the broad bands at $3450\text{--}3300\text{cm}^{-1}$ in Schiff's base. Additionally, the presence of the azomethine $\text{CH}=\text{N}$ stretching at about $1529\text{--}1655\text{cm}^{-1}$ depending on the nature of R side chain substituents, indicates the formation of the Schiff base compounds. The FTIR spectrum of the compound NMH01 showed a stretched band around $3200\text{--}3570\text{ (O-H) cm}^{-1}$, which is attributed to the intramolecular hydrogen bond of the hydroxyl group. Furthermore, compound NHM01 exhibits absorption bands at $1675\text{--}1619\text{cm}^{-1}$ corresponding to the $\text{C}=\text{C}$ and $\text{C}=\text{O}$, respectively. Additionally,

the band at $1446\text{--}1450\text{--}1577\text{ cm}^{-1}$ corresponds to $\text{C}=\text{C}$ of compounds NHM06, NHM04 and NMH11, respectively.

DNA binding studies

UV Absorbance Spectra

UV-spectroscopy being an important qualitative and quantitative analysis technique has been exploited to investigate the interaction of ligands with DNA. The electronic absorption spectrum of DNA exhibits a broad band in the range of $200\text{--}350\text{nm}$ and shows maximum absorption at $\sim 260\text{nm}$. This maximum is a consequence of chromophoric groups in purine and pyrimidine moieties responsible for the electronic transitions (González-ruiz *et al.*, 2011). Therefore, the changes in the absorption spectra of the compound alone and compound-DNA mixture is an indication of DNA-compound interaction, and the mode and strength of binding can also be determined from the shift. The absorbance spectra of DNA could show hypochromism (decreased absorbance intensity) and hyperchromism (increased absorbance intensity) upon titration with the ligand. In general, the intercalative mode of binding usually results in hypochromism and a red-shift because of the strong stacking interaction between an aromatic chromophore and the nitrogen bases of DNA. This results in structural changes of the DNA that entailed the local unwinding of the double helix. Whereas for weak interaction such as hydrogen bonding, groove binding and electrostatic interaction no significant shift of the absorption maxima occurs (Banerjee *et al.*, 2016). The absorption spectra resulting from titrations are depicted in Fig. 2. As observed from spectral curves, the complexes showed pronounced hypochromism with a slight red shift of 2nm . The results suggest that these compounds bind to DNA through an intercalation mode.

The resultant hypochromic effect was found to be 0.244nm for NMH01, 0.201nm for NHM04, 1.53nm for NMH06, and 1.42nm for NMH11 followed by a red shift of magnitude 2.01nm , 1.89nm , 1.73nm and 1.88nm for NMH01, NHM04, NMH06, and NMH11, respectively.

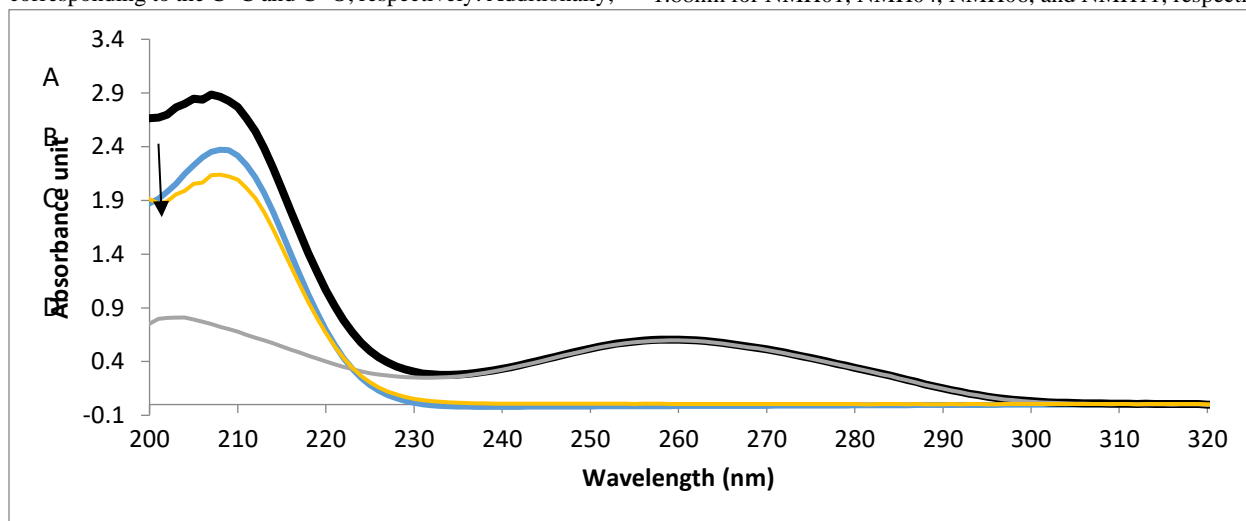


Figure 2: UV-Vis absorption spectra of DNA in the absence and presence of NMH01 (A) the G-DNA-NMH01 complex, (B) the $30\ \mu\text{M}$ NMH01, (C) G-DNA-NMH01 complex subtracted from the G-DNA absorbance to show the hypochromic shift (D) GDNA alone. The experiment was conducted in Tris buffer solution (0.01M Tris, 0.1M NaCl, at pH 7.4). Genomic DNA was used in a concentration of $75\ \mu\text{g/ml}$ and NMH01 $30\ \mu\text{M}$.

Ethidium bromide (EB) Competition Assay

A competitive displacement assay was conducted to obtain further evidence of the binding pattern of the tested compounds and DNA. Ethidium bromide (EB) is a strong fluorescent dye, known to bind to

DNA through intercalation with maximum emission at 661 nm upon binding to double stranded DNA. Free Ethidium bromide exhibits very low fluorescence. However, with the addition of DNA, due to its intercalation, the fluorescence intensity magnifies remarkably (Zhao *et*

et al., 2013). The gradual addition of compounds 1, 4, 6, and 11 to the EB-DNA complex cause a decrease of the emission (quenching effect) (Figure 3). The hypochromic shift appears as a result of formation of a complex between compound and DNA and this reduction of the fluorescence intensity is a characteristic sign of intercalation. The fluorescence spectra of the EB-DNA complex in the absence and presence of NMH01 is shown in Fig. 3. The figure shows that the fluorescence intensity of EB-DNA can be quenched significantly by gradual addition of NMH01. This result indicates that NMH01 was able to replace EB in the DNA helix indicating an intercalative NMH01 DNA binding mode.

The fluorescence quenching data were analyzed by the Stern–Volmer equation and the quenching constants (K_{sv}) were calculated in which the synthesized compounds were the quenchers:

$$I_0/I = 1 + K_{SV} [Q] \quad (1)$$

I_0 and I represent the fluorescence intensities in the absence and presence of quencher, respectively; K_{SV} is the linear Stern–Volmer quenching constant; Q is the concentration of quencher. The K_{SV} values were given by the ratio of the slope to intercept. The K_{SV} value suggests a strong affinity of the compounds to EB-bound G-DNA and that it can competitively displace EB from DNA *via* an intercalative mode of binding. As shown in Table 8, compound NMH01 had the highest K_{SV} value suggesting that compound NMH01 bound most strongly to G-DNA even more than daunorubicin. The K_{SV} values for the tested compounds are listed in Table 8.

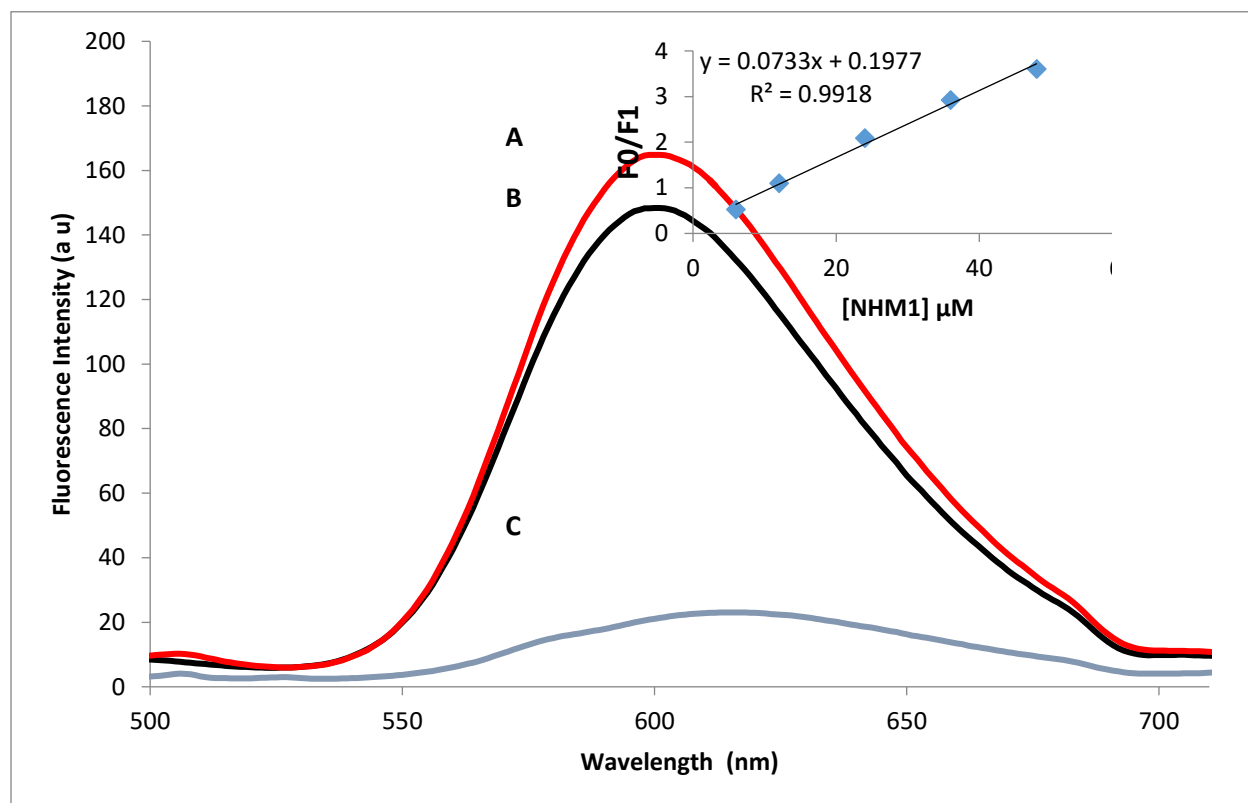


Figure 3. Fluorescence changes of the NMH01 system that contains (A) the G-DNA-ethidium bromide complex, (B) the G-DNA-ethidium bromide complex with 30 μM NMH01 and (C) ethidium bromide alone. The experiment was conducted in Tris buffer solution (0.01M Tris, 0.1M NaCl, at pH 7.4), $\lambda_{\text{ex}} = 480 \text{ nm}$. Inset: plot of F_0/F_1 versus different concentrations of NMH01 (μM) for the titration of NMH01 to G-DNA-EB complex. Genomic DNA was used in a concentration of 75 $\mu\text{g/ml}$ and ethidium bromide 72 μM .

Based upon the variation in absorbance and the fluorescence intensities the binding constant for the compounds to determine the strength of the interaction of compounds with DNA at 298 K, was determined from fluorescence titration data using the Benesi–Hildebrand (BH) equation:

$$1/\Delta A = 1/(K_b \Delta A_0) [\text{DNA}] + 1/(\Delta A_0) \dots \dots (2)$$

Here, the difference in fluorescence was denoted by ΔA , ΔA_0 is maximum fluorescence intensity change and $[\text{DNA}]$ is the concentration of DNA. By plotting the reciprocal of the difference in fluorescence intensity against the reciprocal of DNA concentration, the Benesi–Hildebrand plot was constructed. To determine the extent of DNA-binding affinities of compound towards G-DNA, the intrinsic binding constant (K_b) values were obtained from the linear regression plots of $[1/(\Delta A_0)]$ vs. $\{1/[\text{DNA}]\}$ M^{-1} , and the ratio of the slope to intercept calculated. The K_b binding

constants of compounds are given in Table 8 (Benesi & Hildebrand, 1949).

The Schiff's base derivatives of *o*-phenylenediamine compounds showed similar binding constants and these are close to the binding affinity of the intercalating agent daunorubicin ($7.2 \times 10^4 \pm 0.004 \text{ M}^{-1}$), which agrees well with those reported in the literature ($7.8 \times 10^4 \text{ M}^{-1}$) (Hajian *et al.*, 2009). The overall measured K_b findings for all compounds were in the subsequent sequence: 1 > 4 > 6 > 11. They were within the range of the intercalation mode ($K = 1 \times 10^5 \times 10^{11} \text{ M}^{-1}$), where intercalative mode of interactions had been assigned (Wolfe *et al.*, 1987; Zhou *et al.*, 2016).

The free energy (ΔG) was calculated by using equation $\Delta G RT = - \ln K$ (3), where ΔG is the Gibbs free energy, R is the universal gas constant

(taken as 2cal/mol K), T is the absolute temperature (298 K), and K is the binding constant. The observed values of ΔG were in the range of -6.12 to -6.44 kcal/mol⁻¹ (Table 8), which also indicates that the compounds

spontaneously intercalate to DNA. Compound (NHM01) exhibited the most excellent binding potency compared to others.

Name	KSV (M ⁻¹)	K _a (M ⁻¹)	ΔG kcal mol ⁻¹	R ² (5 points)
Taxol	5.90X10 ³	5.3 X10 ⁴ ±0.002	-6.44	0.99
Daunorubicin	7.91x10 ³	7.2 X10 ⁴ ±0.004	-6.62	0.97
NMH01	9.00X10 ³	5.9 X10 ⁴ ±0.006	-6.50	0.99
NMH04	6.02X10 ³	4.3 X10 ⁴ ±0.001	-6.31	0.98
NMH06	3.02X10 ³	3.9 X10 ⁴ ±0.004	-6.25	0.978
NMH11	2.86X10 ³	3.1 X10 ⁴ ±0.002	-6.12	0.968

Table 8. The key selection vector (KSV) values, the binding constant (K_b) and the free energy (ΔG) of synthesized Schiff's base derivatives of *o*-phenylenediamine.

Conclusion

A new series of fifteen compounds (1-15) possessing *ortho*-phenylenediamine Schiff's base scaffold were designed. Next, ADMET studies were conducted by using SwissADME software and all produced compounds satisfied the Lipinski criterion. Furthermore, the results of docking studies revealed that the docked compounds displayed strong binding affinity with DNA and have a similar binding mode to that of daunorubicin (DNA intercalating agent used as reference) with binding energies ranging from -6.3 to -10.9 kcal/mol. Among all these compounds, four compounds (NMH01, 04, 06, and 11) have been synthesized and characterized by FT-IR, ¹H and ¹³C NMR spectroscopy. The interaction of these compounds with genomic-DNA (G-DNA) has been explored by using absorption spectral and fluorescence displacement studies using ethidium bromide. The results indicate that the compounds bind strongly to G-DNA via an intercalation mechanism. NHM01 showed the highest key selection vector (KSV) value, suggesting that compound NHM01 binds most tightly to G-DNA. Therefore, NHM01, NHM04, NHM06 and NMH11 are proposed as effective cytotoxic agents with potential DNA intercalation and may serve as lead compounds for the discovery of new anticancer agents. Further biological evaluations are necessary to confirm our findings.

Acknowledgement:

We gratefully acknowledge Garabolle Research Center (GRC) for performing FTIR study.

Conflict of interest

The authors declare that the research was conducted in the absence of any commercial or financial relationship that could be construed as a potential conflict of interest and is compliant with ethical standards.

Ethical approval: This article does not contain any studies with human participants performed by any of the authors.

Reference

- Adelusi, T. I., Oyedele, A. Q. K., Boyenle, I. D., Ogunlana, A. T., Adeyemi, R. O. et al. (2022). Molecular modeling in drug discovery. *Informatics in Medicine Unlocked*, 29, 100880. <https://doi.org/10.1016/J.IMU.2022.100880>
- Alam, S., Verma, S., Fatima, K., Luqman, S., Srivastava, S. K. et al. (2023). Pharmacophore & QSAR Guided Design, Synthesis, Pharmacokinetics and In vitro Evaluation of Curcumin Analogs for Anticancer Activity. *Current Medicinal Chemistry*, 31(5), 620–639. <https://doi.org/10.2174/0929867330666230428162720>
- Ali, S. (2013). *Drug – DNA interactions and their study by UV – Visible , fluorescence spectroscopies and cyclic voltametry*. 124(July), 1–6.
- Almaqwashy, A. A., Paramanathan, T., Rouzina, I., & Williams, M. C. (2016). Mechanisms of small molecule–DNA interactions probed by single-molecule force spectroscopy. *Nucleic Acids Research*, 44(9), 3971. <https://doi.org/10.1093/NAR/GKW237>
- Banerjee, A., Singh, J., & Dasgupta, D. (2016). *Fluorescence Spectroscopic and Calorimetry Based Approaches to Characterize the Mode of Interaction of Small Molecules with DNA*. *Fluorescence Spectroscopic and Calorimetry Based Approaches to Characterize the Mode of Interaction of Small Molecules with DNA*. March. <https://doi.org/10.1007/s10895-013-1211-0>
- Benesi, H. A., & Hildebrand, J. H. (1949). A Spectrophotometric Investigation of the Interaction of Iodine with Aromatic Hydrocarbons. *Journal of the American Chemical Society*, 71(8), 2703–2707. https://doi.org/10.1021/JA01176A030/ASSET/JA01176A030.FP.PNG_V03
- Bhaduri, S., Ranjan, N., & Arya, D. P. (2018). An overview of recent advances in duplex DNA recognition by small molecules. *Beilstein Journal of Organic Chemistry*, 14, 1051–1086. <https://doi.org/10.3762/bjoc.14.93>
- Biebricher, A. S., Heller, I., Roijmans, R. F. H., Hoekstra, T. P., Peterman, E. J. G., & Wuite, G. J. L. (2015). The impact of DNA intercalators on DNA and DNA-processing enzymes elucidated through force-dependent binding kinetics. *Nature Communications*, 6, 1–25. <https://doi.org/10.1038/ncomms8304>
- Binaschi, M., Bigioni, M., Cipollone, A., Rossi, C., Goso, C. et al. (2001). Anthracyclines: selected new developments. *Current Medicinal Chemistry. Anti-Cancer Agents*, 1(2), 113–130. <https://doi.org/10.2174/1568011013354723>
- Dahlem Junior, M. A., Nguema Edzang, R. W., Catto, A. L., & Raimundo, J. M. (2022). Quinones as an Efficient Molecular Scaffold in the Antibacterial/Antifungal or Antitumoral Arsenal. *International Journal of Molecular Sciences*, 23(22). <https://doi.org/10.3390/IJMS232214108>
- Daina, A., Michielin, O., & Zoete, V. (2017). SwissADME: A free web tool to evaluate pharmacokinetics, drug-likeness and

- medicinal chemistry friendliness of small molecules. *Scientific Reports*, 7, 1–22. <https://doi.org/10.1038/srep42717>
12. El-Adl, K., El-Helby, A. G. A., Sakr, H., & Elwan, A. (2020). Design, synthesis, molecular docking and anti-proliferative evaluations of [1,2,4]triazolo[4,3-a]quinoxaline derivatives as DNA intercalators and Topoisomerase II inhibitors. *Bioorganic Chemistry*, 105(December), 1–7. <https://doi.org/10.1016/j.bioorg.2020.104399>
13. González-ruiz, V., Olives, A. I., Martín, M. A., Ribelles, P., Ramos, M. T. et al. (2011). *An Overview of Analytical Techniques Employed to Evidence An Overview of Analytical Techniques Employed to Evidence Drug-DNA Interactions . Applications to the Design of Genosensors. January.* <https://doi.org/10.5772/13586>
14. Hajian, R., Shams, N., & Parvin, A. (2009). DNA-binding studies of daunorubicin in the presence of methylene blue by spectroscopy and voltammetry techniques. *Chinese Journal of Chemistry*, 27(6), 1055–1060. <https://doi.org/10.1002/CJOC.200990176>
15. Hamil, A. M., Khalifa, K. M., Al-Houni, A., & El-Ajaily, M. M. (2009). *synthesis, spectroscopic investigation and antiactivity activity of schiff base complexes of cobalt (ii) and copper (II) ions.* 2(2), 261–266. <http://www.rasayanjournal.com>
16. Jing, X., Hou, Y., Hallett, W., Sahajwalla, C. G., & Ji, P. (2019). Key Physicochemical Characteristics Influencing ADME Properties of Therapeutic Proteins. *Advances in Experimental Medicine and Biology*, 1148, 115–129. https://doi.org/10.1007/978-981-13-7709-9_6
17. Koll, A. (2003). Specific Features of Intramolecular Proton Transfer Reaction in Schiff Bases. *International Journal of Molecular Sciences 2003, Vol. 4, Pages 434-444*, 4(7), 434–444. <https://doi.org/10.3390/I4070434>
18. Lipinski, C. A., Lombardo, F., Dominy, B. W., & Feeney, P. J. (2001). Experimental and computational approaches to estimate solubility and permeability in drug discovery and development q settings. *Advanced Drug Delivery Reviews*, 46, 3–26. www.elsevier.com/locate/drugdeliv
19. Lucaciu, R. L., Hangan, A. C., Sevastre, B., & Oprean, L. S. (2022). Metallo-Drugs in Cancer Therapy: Past, Present and Future. *Molecules*, 27(19), 1–40. <https://doi.org/10.3390/molecules27196485>
20. Mohamed, A., & S.N, M. (2021). Swiss ADME predictions for anti cancer drug molecules prior In Vitro In Vivo Correlations (IVIVC). *Jiangsu Daxue Xuebao (Ziran Kexue Ban) / Journal of Jiangsu University (Natural Science Edition)*, 17(07), 142–169.
21. Morak-Młodawska, B., Jeleń, M., Martula, E., & Korlacki, R. (2023). Study of Lipophilicity and ADME Properties of 1,9-Diazaphenothiazines with Anticancer Action. *International Journal of Molecular Sciences*, 24(8), 1–17. <https://doi.org/10.3390/ijms24086970>
22. Navarro-Tovar, G., Vega-Rodríguez, S., Leyva, E., Loredó-Carrillo, S., de Loera, D., & López-López, L. I. (2023). The Relevance and Insights on 1,4-Naphthoquinones as Antimicrobial and Antitumoral Molecules: A Systematic Review. *Pharmaceuticals*, 16(4). <https://doi.org/10.3390/PH16040496>
23. Peng, Y., Zhong, H., Chen, Z. F., Liu, Y. C., Zhang, G. H. et al. (2014). A planar Schiff base platinum(II) complex: Crystal structure, cytotoxicity and interaction with DNA. *Chemical and Pharmaceutical Bulletin*, 62(3), 221–228. <https://doi.org/10.1248/cpb.c13-00256>
24. Savjani, K. T., Gajjar, A. K., & Savjani, J. K. (2012). Drug Solubility: Importance and Enhancement Techniques. *ISRN Pharmaceutics*, 2012, 1–10. <https://doi.org/10.5402/2012/195727>
25. Senthil Kumar Raju, Archana Settu, Archana Thiyagarajan, Divya Rama, Praveen Sekar. et al. (2022). Biological applications of Schiff bases: An overview. *GSC Biological and Pharmaceutical Sciences*, 21(3), 203–215. <https://doi.org/10.30574/gscbps.2022.21.3.0484>
26. Serec, K., Dolanski Babí, S., Podgornik, R., & Tomí, S. (2016). Effect of magnesium ions on the structure of DNA thin films: an infrared spectroscopy study. *Nucleic Acids Research*, 1. <https://doi.org/10.1093/nar/gkw696>
27. Vernekar, B. K., & Sawant, P. S. (2023). Interaction of metal ions with Schiff bases having N2O2 donor sites: Perspectives on synthesis, structural features, and applications. *Results in Chemistry*, 6, 101039. <https://doi.org/10.1016/J.RECHEM.2023.101039>
28. Wadler, S., Tenteromano, L., Cazenave, L., Sparano, J. A., Greenwald, E. S. et al. (1994). Phase II trial of echinomycin in patients with advanced or recurrent colorectal cancer. *Cancer Chemotherapy and Pharmacology*, 34(3), 266–269. <https://doi.org/10.1007/BF00685088/METRICS>
29. Wolfe, A., Shimer, G. H., & Meehan, T. (1987). Polycyclic aromatic hydrocarbons physically intercalate into duplex regions of denatured DNA. *Biochemistry*, 26(20), 6392–6396. <https://doi.org/10.1021/BI00394A013>
30. Zhao, J., Li, W., Ma, R., Chen, S., Ren, S. et al. (2013). *Design , Synthesis and DNA Interaction Study of New Potential DNA Bis-Intercalators Based on Glucuronic Acid.* 16851–16865. <https://doi.org/10.3390/ijms140816851>
31. Zhou, X. Q., Li, Y., Zhang, D. Y., Nie, Y., Li, Z. J. et al. (2016). Copper complexes based on chiral Schiff-base ligands: DNA/BSA binding ability, DNA cleavage activity, cytotoxicity and mechanism of apoptosis. *European Journal of Medicinal Chemistry*, 114, 244–256. <https://doi.org/10.1016/J.EJMECH.2016.02.055>



This work is licensed under Creative Commons Attribution 4.0 License

To Submit Your Article Click Here:

Submit Manuscript

DOI:[10.31579/2690-1897/209](https://doi.org/10.31579/2690-1897/209)

Ready to submit your research? Choose Auctores and benefit from:

- fast, convenient online submission
- rigorous peer review by experienced research in your field
- rapid publication on acceptance
- authors retain copyrights
- unique DOI for all articles
- immediate, unrestricted online access

At Auctores, research is always in progress.

Learn more <https://auctoresonline.org/journals/journal-of-surgical-case-reports-and-images>